THESIS FOR THE DEGREE OF LICENTIATE OF ENGINEERING

Upscaling and Evaluation of Absorption Based Systems for Co-removal of NO_x and SO_x from Flue Gases

JAKOB JOHANSSON

Department of Space, Earth and Environment
Division of Energy Technology
CHALMERS UNIVERSITY OF TECHNOLOGY

Gothenburg, Sweden 2020

Upscaling and Evaluation of Absorption Based Systems for Co-removal of NO_x and SO_x from Flue
JAKOB JOHANSSON

Department of Space, Earth and Environment
Division of Energy Technology
Chalmers University of Technology
SE-412 96 Gothenburg
Sweden
Telephone + 46 (0)31-772 1000

Printed by Chalmers Reproservice
Chalmers University of Technology
Gothenburg, Sweden 2020

Upscaling and Evaluation of Absorption Based Systems for Co-removal of NO_x and SO_x from Flue Gases

JAKOB JOHANSSON
Department of Space, Earth and Environment
Division of Energy Technology
Chalmers University of Technology

Abstract

As long as combustion remains a vital part of the energy system, the removal of nitrogen oxides (NO_x) will be a challenge that will need to be addressed. In addition, emissions of sulfur oxides (SO_x) will be a problem as long as fuels such as coal and oil are used, as is envisaged in every road map suggested by the Intergovernmental Panel on Climate Change (IPPC). With stricter emission regulations being enforced across all fields, new technologies that are adapted to the circumstances will be required to keep costs down. A promising concept for lowering cost involves the removal of several impurities within the same unit, with the co-removal of NO_x and SO_x being one of the most intensively researched applications.

This thesis covers three studies that are focused on the concept of co-removal of NO_x and SO_x in a wet scrubber unit, whereby the NO is oxidized to NO_2 by the introduction of an oxidizing agent, ClO_2, into the flue gas stream before the scrubber. The oxidation of NO to NO_2 by ClO_2 has been tested for a wide variety of flue gas compositions and temperatures, applying a total of three intermediate scales: 0.2 Nm^3/h with synthetic flue gases, 100 Nm^3/h with flue gases from a propane flame, and a ~400 Nm^3/h slip stream from a waste-fired power plant. An efficient NO to NO_2 oxidation was observed at all scales with complete conversion at a ClO_2/NO ratio of ~0.5. No interaction between ClO_2 and SO_2 was observed.

In terms of the absorption process, a number of liquid compositions has been tested at each scale, showing that the concentrations of SO_2 and NO_2 in the flue gas can both be reduced to a few ppm. However, the rate of NO_2 removal is strongly dependent upon the presence of S(IV) in the absorbing liquid. The derived model gives good agreement with the experimental outcomes for the 100 Nm^3/h and 400 Nm^3/h setups, without any extensive parameter fitting. The most important discrepancy noted in relation to the understanding of the associated chemistries is the rate of S(IV) oxidation in the scrubber tower. The work of this thesis represents the first validation of the concept and methodology of scale-up of the co-removal process, and paves the way for commercialization.

Keywords: Emissions control, NO_x, SO_x, ClO_2, absorption, scale-up, gas-phase oxidation

List of Publications

This thesis is based on the following papers, which are referred to in this thesis according to their Roman numerals:

I. Johansson, J.; Hulten, A. H.; Ajdari, S.; Nilsson, P.; Samuelsson, M.; Normann, F.; Andersson, K., *Gas-Phase Chemistry of the NO-SO_2-ClO_2 System Applied to Flue Gas Cleaning.* Industrial & Engineering Chemistry Research 2018, 57, (43), 14347-14354.

II. Johansson, J.; Normann, F.; Sarajlic, N.; Andersson, K., *Technical-scale Evaluation of Scrubber-based, Co-Removal of NO_x and SO_x Species from Flue Gases via Gas-Phase Oxidation*. Industrial & Engineering Chemistry Research 2019, 58, (48), 21904-21912.

III. Johansson, J.; Hulten, A. H.; Normann, F.; Andersson, K., *Co-Removal of NO_x and SO_x. Scale-Up, Experiments and Simulations.* Submitted for publication.

Jakob Johansson, who is the main author of all three papers, was responsible for the experimental work and data evaluation in all the papers, as well as for the modeling work in **Paper II** and **Paper III**. Associate Professor Fredrik Normann and Professor Klas Andersson contributed with discussions and editing for all the papers. Dr. Sima Ajdari conducted the NO_2-SO_2 experiments and modeling in **Paper I**. Nadine Sarajlic contributed to the modeling in **Paper II**. Dr. Anette Heijnesson-Hultén, Pär Nilsson and Marie Samuelsson took part in the experiments described in **Paper I**. Dr. Anette Heijnesson-Hultén also contributed to the experiments described in **Paper III**, as well as to the editing of the paper.

Acknowledgments

First, I would like to express my gratitude to Nouryon, Nordic Energy Research and *Energimyndigheten* for supporting this work financially. I also thank the team at Nouryon, Anette, Pär and Marie, who have played a vital role in this work since day one.

I would like to express my appreciation to the research engineers at Chalmers *Kraftcentral* - you have all assisted me in one way or another - and special thanks to Johannes Öhlin who has been there during the experiments, teaching me, keeping things in order, and always with a smile. Thanks to the A-Team for helping with everything.

A large thank you to my supervisor, Klas Andersson. Without the discussions we had during my Master's thesis work, I would not have even considered going into academia, but you have a way to inspire people. To all my colleagues at Energy Technology, you are the other reason why I applied for this position. This working place is truly fantastic in having so many great colleagues. A special shout out to Adrian Gunnarsson - thank you for taking time to help with my experiments, even when you had so much on your own plate.

Daniel Bäckström, you defined my first time here as a Ph.D. student. You helped me with my first experiments and taught me everything I know about the 100-kW unit. The quality of the initial work is a lot higher thanks to you.

Another important piece of the work puzzle is Fredrik Normann. You have invested tremendous effort into this work and into my first three years as a Ph.D. student. Without you, this would not have been possible. You are a source of information and inspiration and your door is always open, for which you have my deepest thanks.

Finally, I want to thank all those persons outside Chalmers who mean the world to me. My fantastic friends, my wonderful family and the love of my life, Julia. Life is so much more than just work and you are the most important part of it. Thank you!

Jakob Johansson
Gothenburg, Sweden, 2020

Table of Contents

CHAPTER 1

Introduction

Air pollution is a serious environmental issue with direct effects on human health. Energy conversion is the major source of emissions.[1] The growing global population and increasing economic standards provide a stark choice of increased primary energy usage or comprehensive lifestyle changes.[2] Figure 1 shows that, historically, regulations that target specific point sources of emissions have been very successful in achieving drastic decreases in specific emissions.[3] However, with the easily achieved decreases in emission already pushing current technological boundaries, further reductions in emissions will have to come from regulating emissions sources that have not previously been considered. Such emission sources include emissions from manufacturing industries and medium-scale sources.

Conventional flue gas cleaning techniques might not be directly applicable or too expensive to implement to the conditions of these new emission sources depending on the technology used. To continuously reduce emission levels without having a negative impact on the competitiveness of the concerned industry, more efficient cleaning technologies are needed on an ongoing basis. Flue gas cleaning is as important today as it has been since the 1970's when the environmental effects of air pollution first became a global concern.

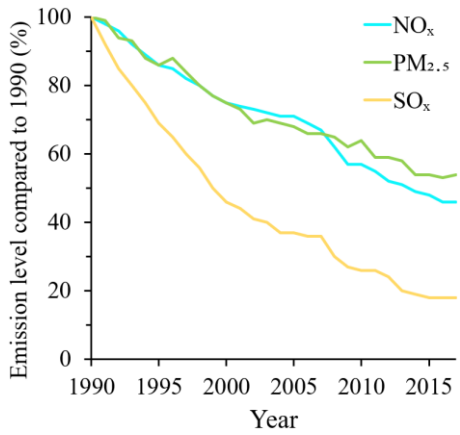

Figure 1: Comparison of yearly emission levels in all EEA-33 countries to the levels in 1990 for three major pollutants: nitrogen oxides (NO_x), particulate matter sub-2.5 microns ($PM_{2.5}$), and sulfur oxides (SO_x). Data taken from the EEA database.[3]

1.1 Aim

This thesis investigates a specific flue gas cleaning concept for the removal of nitrogen oxides (NO_x) and sulfur oxides (SO_x) in one and the same unit, with the aim of reducing costs and the area requirement. The work combines experimental studies with modeling runs. The experimental work is mainly performed to develop and demonstrate process performance. Modeling is used for the evaluation of the experimental results, and to predict the impact of the final concept. Three main areas are investigated:

- The efficiency of ClO_2 as an oxidizing agent for gas-phase oxidation of NO to NO_2.
- The performance of the liquid-phase chemistry in a combined SO_x-NO_x scrubbing system.
- A method for efficient verification and up-scaling of the technology.

1.2 Outline of the Thesis

The thesis consists of an introductory essay in which the work is place in the context of current knowledge, the main theory behind the proposed concept is introduced, and the methodology is described. The Background section concludes with the key findings from the work and proposes a way forward. The thesis is based on the three appended papers, which are summarized below.

Paper I is an experimental investigation of the gas-phase interactions between NO, SO_2 and ClO_2.

Paper II is an experimental investigation of the simultaneous absorption of SO_x and NO_x at technical scale. **Paper II** also describes the first validation of the previously proposed state-of-the-art reaction mechanism of the liquid-phase chemistry of a SO_x/NO_x scrubber system.

Paper III compares the performances of three scales of the co-removal system used in the work and discusses the up-scaling of the concept. This paper includes experimental results, as well as the outcomes of the process modeling.

CHAPTER 2

Background

2.1 Air Pollution

Air pollution is a major environmental concern. Ambient air pollution may be divided into four major categories according to the World Health Organization (WHO): particulate matter (PM); ground-level ozone; nitrogen oxides (NO_x); and sulfur oxides (SO_x). All of these are products, directly or indirectly, of combustion.[4] For the effect of any of these emissions to be acute, the concentrations need to be very high, often higher than what can be accumulated in a ventilated area. Instead, the danger lies in long-term exposure to pollutants.[5] The WHO estimates that 7.6% of all deaths worldwide in 2016 were related to the above mentioned ambient air pollution.

Since combustion is the major source of all these emissions, one might ask why humanity isn´t switching to a different way of converting energy. The answer is simply that the primary energy sources accessed through combustion represent either the simplest or cheapest way of converting energy and often use infrastructure that is already in place. Globally, we are consuming energy at a level that is difficult, if not impossible, to supply with current primary energy sources, excluding fuels for combustion. Figure 2 shows the distribution in global primary energy supply. In 2018, around 10% of the global primary energy supply originated from sources that are considered "free" of direct ambient air pollutants (hydroelectricity, nuclear energy and renewables, excluding biomass). Even though wind and solar power generation is increasing rapidly, it is currently outpaced by the total level of energy consumption. These trends and the order of magnitude of combustion motivate exploration of the potential of flue gas cleaning, not only in terms of its application only today but also its value for generations to come. This work focuses on the cleaning of NO_x and SO_x from gas emissions sources.

Emissions of NO_x have been established as a source for the formation of ozone, smog and acid rain. Smog or 'smoky fog' may form from emissions in populated areas. The original type of smog, which was more common before 1960 but remains a problem in some parts of the world, was formed from direct emissions originating from incomplete combustion, most commonly of coal. This type of smog is especially common during winter inversions when emissions levels are higher and tend to accumulate at ground level. The type of smog that is more commonly observed today, known as photochemical smog, involves chemical reactions between NO_x and hydrocarbons in the atmosphere and is enhanced by radiation from the sun, forming a number of harmful chemicals. Photochemical smog is a major problem in many large cities around the world, such as Beijing, Los Angeles and Mexico City.

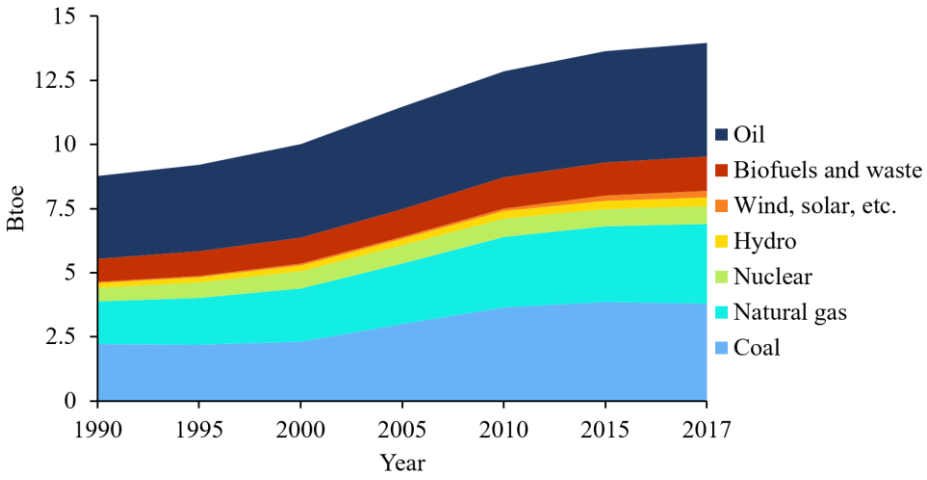

Figure 2: Total global primary energy supply divided by source, from 1990 to 2017 in billion tonne of oil equivalents (Btoe). Data from the IEA Policies and Measures Database © OECD/IEA.[6]

Acid rain, while not directly harmful to humans, is still a concern in many places around the world. Acid rain refers to rain that has an increased number of hydrogen ions, produced from reactions with SO_x and NO_x. Acid rain can as such have a direct impact on the pH levels of lakes and other wetlands. Many plants and even animals are not adapted to changes in pH, and acid rain is the reason for extinction of life in many lakes. In cities, acid rain causes corrosion and deterioration of structures, especially those made of marble or limestone, as these materials are rich in calcium and reacts with the acids.

Since the downside of emitting SO_x and NO_x is well-established, regulations have for several decades pushed for the development of reduction technologies. Currently, it is possible to remove sulfur from liquid and gaseous fuels before combustion, reduce the amount of NO_x formed during combustion, and capture the SO_x and NO_x from the flue gases. These technologies may, however, not be optimal for all types of emissions sources. As the regulations start to affect a wide variety of industries and end-users, new and tailored technologies are needed to maintain competitiveness.

2.2 Conventional NO_x Control

The most commonly used secondary measures to control NO_x emissions are selective catalytic reduction (SCR) and selective non-catalytic reduction (SNCR). Both processes utilize urea or ammonia to reduce NO to N_2. In SCR, a catalyst is used to lower the activation energy of the reaction and increase the chemical reduction of NO. SCR is usually operated at temperatures in the range of 300°–400°C. In SNCR, in which no catalyst is used, a temperature in the range of 800°–1100°C is needed to reduce NO, which is why the reducing agent

is often introduced to the flue gas in close proximity to the combustion chamber.

SCR is considered a best-available technology (BAT) for NO_x control in large combustion plants. The reduction of NO can be substantial depending on the amount of reducing agent used. Strict regulations regarding ammonia slip require stringent control of the process. One of the major drawbacks of the process is the cost, with the reducing agent, noble metal catalyst, and often the requirement for additional heating all having significant impacts on the running and capital costs.

SNCR is considered a BAT for large combustion plants with lower levels of NO_x production. The avoided cost of a catalyst and direct injection of the reducing agent into the furnace means a reduced capital cost, although this results in a much lower reduction potential. SNCR reduces around 50% of the NO to N_2. The lower reaction rate of non-catalytic reduction requires a larger amount of reduction agent to be injected, as compared to SCR. The unreacted reduction agent will, together with other impurities in the flue gas, form deposits on surfaces downstream, causing corrosion and plugging and lower heat transfer.

2.3 Conventional SO_x Control

The removal of sulfur from flue gases may be performed with high efficiency for most applications. The removal often includes calcium, which reacts with sulfur to form stable sulfates. The process can be wet or dry with production of the byproduct gypsum, which is used as a construction material or landfill. The large amount of gypsum produced from wet flue gas desulfurization (FGD) has resulted in market saturations, with consequent drop in price. This may, however, change as increasing demand is expected.[7] FGD using a limestone slurry is considered a BAT for most large combustion plants. If limestone is readily available close to the site, wet FGD has a relatively low running cost. although it requires large areas for installation and waste disposal.[8]

2.4 Co-removal of NO_x and SO_x

The conventional flue gas cleaning measures may be approaching the limit of their usefulness in terms of realizing further increases in removal and cost efficiencies. One approach to reducing significantly the size and cost of the equipment is to control both SO_x and NO_x in the same unit. While this concept has been explored to various extents for several years, it has in recent years gained momentum in connection with the development of pressurized flue gas systems for carbon capture and storage (CCS) systems.[9-12]

In CCS schemes, as the temperature decreases and pressure increases, water in the flue gas will condense and react with SO_2/SO_3 to form sulfuric acid, creating a way for passive SO_x removal. At the same time, the raised pressure increases the oxidation rate of NO to NO_2 which increase the solubility in water

of the NO_x. The increased pressure by such enables removal of both NO_x and SO_x though condensation and absorption in the flue gas path.

In an atmospheric pressure system, the oxidation of NO to NO_2 is far too slow to be of relevance for flue gas cleaning applications without complementary measures. The formation of NO_2 may be enhanced through the introduction of an oxidizing agent, such as H_2O_2, O_3 or ClO_2.[13-15] After oxidation, simultaneous scrubbing of NO_x and SO_x can be performed. It is on this principle that the process investigated in the present work is based. Figure 3 presents an overview of the discussed process. The efficiency of the NO_x and SO_x scrubber in atmospheric pressure systems is highly dependent upon the established influence of S(IV) on NO_2 absorption.[16, 17] S(IV) will form when SO_2 is absorbed into the liquid and will rapidly and efficiently reduce NO_2 to HNO_2. The synergy in the liquid phase between SO_x and NO_x absorption reveals possibilities for a removal technology that is both process- and cost-efficient.

The concept of simultaneous removal of NO_x and SO_x for flue gas cleaning applications was first proposed in 1973 and has continued to generate interest. Senjo and Kobayashi applied for a patent for the "Process for removing nitrogen oxides from gas" in 1973, in which it is proposed to oxidize NO to NO_2 with ClO_2 or O_3.[9] The intended application was not directly targeted towards simultaneous removal of SO_2, although it is mentioned in the patent as an option.

In subsequent years, many research groups investigated the process or parts of it, with every project concentrating on the oxidation of NO to NO_2. Several groups focused on liquid-phase oxidation of the NO with different oxidizing agents.[10, 18-20] Depending on the agent used, different scrubber pH is required for efficient absorption. There has also been some research on gas-phase oxidation of NO.[20-22] A wide variety of experimental setups have been used with different rates (from 3% to 99%) of removal of NO_x being reported. In contrast, the rate of SO_2 removal is always >80%, using alkaline scrubber solutions.

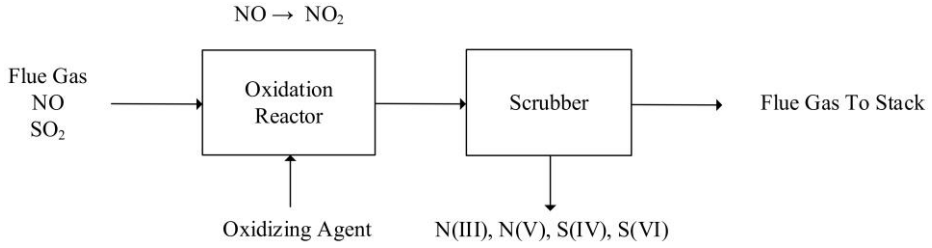

Figure 3: Overview of the discussed concept for simultaneous removal of NO_x and SO_x from flue gases in a process that employs enhanced oxidation of NO.

Some groups have focused on introducing NO_x absorption into specific, existing FGD processes, such as those involving magnesia and limestone slurries.[17, 23] The attention of the reader is directed to the rapid oxidation of S(IV) that takes place in the absorption process.

In the early 2000s, there was increased interest in next-generation combustion technologies for CCS schemes, such as oxy-fuel combustion and chemical looping combustion (CLC). Soon thereafter it was discovered that the presence of SO_x and NO_x caused problems during compression. White et al.[11] proposes a process in which SO_x and NO_x are removed during and after compression in stages; they have provided supporting experimental data and termed this process " the sour compression process". In sour compression, mainly SO_2 will be removed in the first stage and NO_2 in the second stage. The process has been further investigated by other research groups with alternative designs discussed.[12, 24, 25] A detailed reaction mechanism has been developed by our research group at Chalmers, based on a literature review of the possible reactions.[26, 27]

2.5 Concept Applications

Possible applications for the discussed technology include conventional emissions sources with rigorous emission control systems, such as large-scale coal or waste-fired heat and power plants, as well as emissions sources with up-coming requirements for emission control, such as manufacturing industries, medium-sized plants, and maritime transport. However, as flue gas cleaning is a conservative business, it seems more likely that a novel technology will be implemented. Furthermore, the conventional technologies have been long-established, and cost-optimized over many decades, so the competition is therefore considerable. The considered emissions sources and their characteristics of importance for the discussed technology are described below.

Ships - The environmental impact of the global maritime transport system is attracting more attention. Difficulties encountered with implementing regulations that encompass companies acting in international waters have previously seen the sea-freight sector function almost without regulations. This coupled with the fact that ships run on almost a waste product of oil refineries mean that they are major point sources of SO_x and NO_x emissions. Recent directives from the EU restrict the usage of certain oil products in European waters and requires that both NO_x and SO_x is to be cleaned from the flue gases while in harbors.[28] On the global level, the allowed sulfur content of fuels was decreased at the beginning of 2020, and standards for NO_x emissions in certain control zones will be stricter from the start of 2021.[29] The new limit on the sulfur content of fuels is set at 0.5% m/m, which is comparable to the contents of many fuel coals used, or requires implementations of equivalent measures. Since the rate of NO_2 absorption increases with increasing SO_2 concentration,

the dirty maritime fuels appear at first glance to be amenable to co-absorption of NO_x and SO_x.

Manufacturing industry - Pulp and paper manufacturing is a prime candidate for NO_x absorption through gas-phase oxidation. While the flue gases produced in the system are largely lacking in sulfur, sulfur is already present in the system due to the de-lignification step. There is also on-site production of oxidation agents such as ClO_2 from the bleaching step. The pulp and paper industry accounted for approximately 7% of the total emissions from heat and power production in Sweden in 2018, spread across 37 individual plants.[30] The industry presents a large point source with most of the required processes already in place, resulting in relatively low-risk implementation of the NO_2 scrubbing process.

CCS - CCS in general and from biogenic sources in particular, is one of few solutions to meet the 1.5 degree target while not making large changes to the ways in which Society consumes energy.[2] As mentioned previously, CCS requires the flue gas to be pressurized. With an increase in pressure, SO_2, if present, and NO_x will inevitably be absorbed into the condensed flue gas water. Thus, it is imperative that SO_2 and NO_x are removed before the compressors or that the flue gas train is designed in a way that allows control of the absorption process. Pressurized systems will not require the oxidizing agents used in this work, although the liquid-phase chemistry is believed to be the similar between the systems. Therefore, research into one concept will enhance understanding of the other concept.

CHAPTER 3

Chemistry

The concept of concomitant absorption of NO_x and SO_x from flue gases includes two important reaction schemes: 1) the oxidation of NO to NO_2, which increases the solubility of NO_x; and 2) the liquid-phase interactions of the sulfur and nitrogen chemistry, which facilitate efficient absorption. Figure 4 shows a schematic overview of the proposed reaction scheme. The reactions included are those that are deemed to have significance during the experiments. For a more detailed chemistry, see the work of Ajdari et al.[27]

The gas-phase oxidation is here performed with ClO_2 as the oxidizing agent. The oxidation of NO takes place according to Reactions 1 and 2.[31-34] Under dry conditions, Reactions 1 and 2 have a theoretical stoichiometry of 0.5 between NO and ClO_2.

$$NO + ClO_2 \rightarrow NO_2 + ClO \quad (1)$$

$$NO + ClO \rightarrow NO_2 + Cl \quad (2)$$

In the presence of water, ClO_2 may be fully reduced to Cl^-, and the theoretical stoichiometry between NO and ClO_2 will then be 0.4, according to Reaction 3.

$$5NO + 3ClO_2 + 4H_2O \rightarrow 5HNO_3 + 3HCl \quad (3)$$

SO_2 absorption in water is equilibrium-controlled and leads to the formation of bisulfite and sulfite according to Reactions 4 and 5, respectively,[35-38]

$$SO_2(aq) + H_2O(l) \leftrightarrow H^+ + HSO_3^- \quad (4)$$

$$HSO_3^-(aq) \leftrightarrow H^+ + SO_3^{2-} \quad (5)$$

Absorption of NO_2 in water takes place according to either Reaction 6 or 7, depending on the presence of NO and the pH level.[39-41]

$$2NO_2(aq) + H_2O(l) \rightarrow HNO_2(aq) + HNO_3(aq) \quad (6)$$

$$NO + NO_2 + H_2O \leftrightarrow 2HNO_2 \quad (7)$$

Nitrite, N(III), is inherently unstable, especially under acidic conditions, and it can decompose into NO and NO_2:

$$2HNO_2(aq) \leftrightarrow NO(aq) + NO_2(aq) + H_2O \quad (8)$$

Several studies have shown that S(IV) is efficient at hydrolyzing NO_2(aq) at a high rate according to Reaction 9.[42-46]

$$2NO_2(aq) + SO_3^{2-} + H_2O(l) \rightarrow 2NO_2^- + SO_4^{2-} + 2H^+ \quad (9)$$

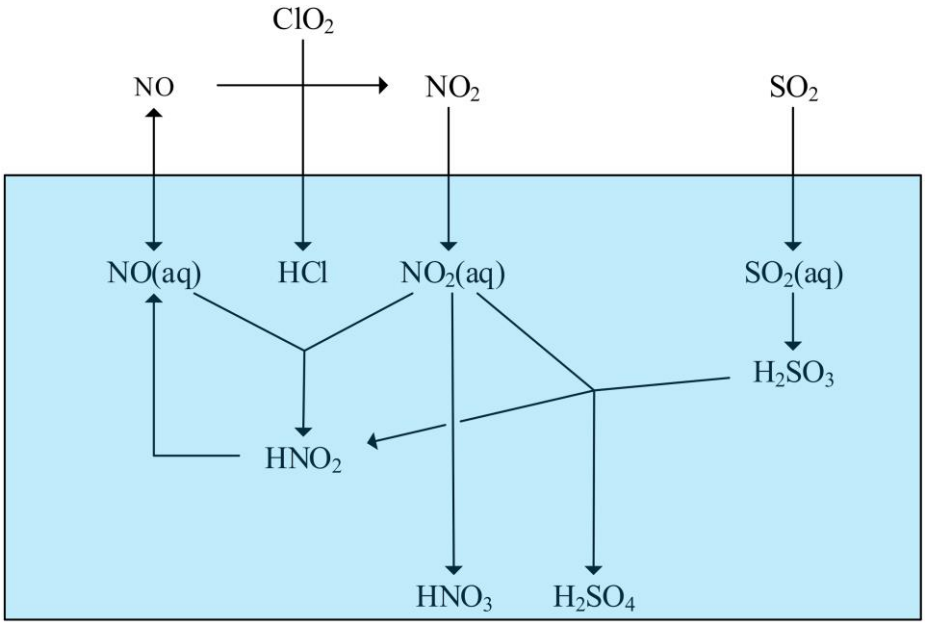

Figure 4: Schematic overview of the chemistry used to describe the simultaneous absorption of NO_x and SO_x after enhanced NO oxidation to NO_2 using ClO_2.

CHAPTER 4

Methodology

This thesis investigates the implementation of a flue gas cleaning concept for simultaneous removal of SO_x and NO_x through gas-phase oxidation of NO to NO_2 using ClO_2, followed by wet scrubbing. The implementation of the concept is evaluated experimentally in steps, following up-scaling of the process, Figure 5 pictures the overall methodology.

The concept was first evaluated in a bench-scale unit, treating 0.2 Nm^3/h of a simulated flue gas flow. Initially, the efficiency of ClO_2 as an efficient oxidizing agent for gas-phase oxidation of NO to NO_2 was established for a wide variety of flue gas temperatures and compositions (**Paper I**). The remainder of the work focused on the efficiency and the implementation of the absorption process. The effects of the pH level, temperature and additives of the absorbing liquid, as well as the flue gas composition formed the main focus.

For the technical-scale testing, the 100-kW oxy-fuel unit at Chalmers was retrofitted with the required flue gas cleaning path. At 100 Nm^3/h, many of the issues related to small-scale scrubbing at 0.2 Nm^3/h are avoided and the technical feasibility may be evaluated. The 100 Nm^3/h unit was used to test the concept for a combustion-derived flue gas, with scrubbing in a purpose-built scrubber and with consideration of safety issues related to the used chemicals. The experimental results represent a first dataset for validation of the reaction mechanism previously proposed by our research group (Ajdari et. al[27]) (**Paper II**).

The 400 Nm^3/h field-testing unit is capable of evaluating the concept at different sites and in a continuous mode of operation. The scrubber unit has a design similar to that of the 100 Nm^3/h unit but offers an automated process control with continuous flows and more measurement points. For these tests, the unit was installed at a waste-to-heat plant where a slipstream of the flue gas was led to the field-testing unit. The 400 Nm^3/h unit allowed the acquisition of new expertise regarding the implementation of the process and process control. Finally, this work summarizes and compares the performance of the process across the scales tested (**Paper III**), leading to a discussion of the up-scaling methodology.

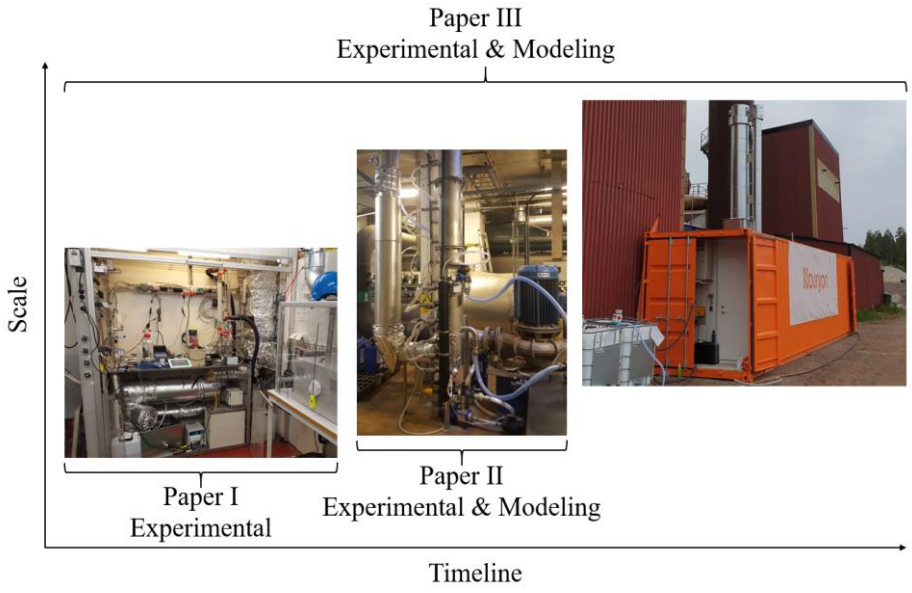

Figure 5: Relationships between the three papers and three experimental setups that constitute the basis for this thesis. Left: 0.2 Nm^3/h setup, Middle: The oxidation reactor and scrubber of the 100 Nm^3/h setup attached to Chalmers 100 kW oxy-fuel combustor, Right: The 12m long container housing the 400 Nm^3/h setup attached with a slip stream from the waste to heat plant Källhagsverken in Avesta.

4.1 Data Evaluation

The evaluation of the results is based on a few key performance indicators, as defined below. The molar ratio between added ClO_2 and the NO after combustion to be oxidized is defined as:

$$r_{ClO2} = \frac{ClO_2}{NO_{pre-oxidation}}. \quad (4.1)$$

The performance of the NO oxidation process is indicated by the NO conversion, which is based on the measured dry concentration of NO before and after the oxidation reactor:

$$\text{NO conversion} = 1 - \frac{NO_{post-oxidation}}{NO_{pre-oxidation}}. \quad (4.2)$$

The amount of NO_x absorption is defined as the rate of reduction of NO_x in the flue gas, which is based on the measured dry concentrations of NO and NO_2 before the oxidation reactor and after the scrubber:

$$NO_x \text{ absorption} = 1 - \frac{NO_{post-scrubber} + NO_{2,post-scrubber}}{NO_{pre-oxidation} + NO_{2,pre-oxidation}}. \quad (4.3)$$

Note that the total amount of NO and NO_2 after the oxidation reactor may be slightly lower than before the reactor due to losses in the pipes, why the NO_x measured before the oxidation reactor is used to evaluate NO_x absorption.

When the specific absorption of NO_2 or NO is evaluated, the dry-basis concentrations before and after the scrubber are used as follows:

$$\mathrm{NO_2\ absorpotion} = 1 - \frac{\mathrm{NO_{2,post-scrubber}}}{\mathrm{NO_{2,post-oxidation}}}, \tag{4.4}$$

$$\mathrm{NO\ absorption} = 1 - \frac{\mathrm{NO_{post-scrubber}}}{\mathrm{NO_{post-oxidation}}}. \tag{4.5}$$

Similar to NO conversion, SO_2 conversion is defined as follows:

$$\mathrm{SO_2\ conversion} = 1 - \frac{\mathrm{SO_{2,post-oxidation}}}{\mathrm{SO_{2,pre-oxidation}}}. \tag{4.6}$$

CHAPTER 5

Experimental

5.1 The 0.2 Nm^3/h Unit

The 0.2 Nm^3/h unit is illustrated in Figure 6. The desired gas compositions are obtained through the mixing of N_2, CO_2, O_2, NO, and SO_2. Water is added in a humidifier. The ClO_2 gas is added to the gas mixture under various process conditions. The flue gas compositions and process conditions used in this study are presented in Table 1.

The gases used in the gas mixing system are: N_2 (100%), CO_2 (100%), O_2 (100%), SO_2 (10% in N_2), and NO (10% in N_2) (all from AGA Linde). The addition of the gases is controlled using Bronkhorst mass flow controllers (MFCs; EL-Flow series). Water vapor is produced by the Bronkhorst controlled evaporation and mixing (CEM) system supplied by Omni Process, Sweden. The water vapor is added to the flue gas stream in close conjunction with the pre-heater, in order to avoid condensation. The pre-heater (made of stainless steel) and reactor system (made of titanium) consists of two pipes that are heated with oil. The pipes are connected by a mixing zone where the ClO_2 gas is added. This system provides a uniform reaction temperature (±1°C) up to a temperature of 300°C. The ClO_2 gas is produced from an aqueous chlorine dioxide solution (ClO_2 gas dissolved in water) by stripping. Nitrogen is allowed to pass through a bubble plate into a flask, thereby releasing ClO_2 gas. The charge of ClO_2 gas is controlled by choosing an appropriate nitrogen flow through an aqueous ClO_2 solution of known concentration at a specified temperature. The temperature is maintained by a water-bath, and the concentration of the solution is continuously determined by circulating the aqueous chlorine dioxide through a spectrophotometer (Hach Lange DR 2800).

After the oxidation reactor, the flue gas enters a scrubber (Günter DIEHM Process Systems, Germany), which is random-packed with Raschig rings measuring 6×6 mm, composed of borosilicate glass, and operating with a counter-flow liquid stream. The absorption solution was recirculated during the trial and the pH level was varied from 1 to 10 by adding 1 M hydrochloric acid (HCl, laboratory grade) or 1 M sodium hydroxide (NaOH, Scharlau, laboratory grade). The flue gas is led via Teflon-lined heated tubes to the Fourier-transform infrared spectroscopy (FTIR) gas analyzer. The gas can also bypass the scrubber, allowing determination of the gas composition after the oxidation reactor. The FTIR is the MKS MultiGas™ 2030, which is capable of measuring NO, NO_2, HNO_3, N_2O, SO_2 and HCl, as well as other less-likely species for the system. Gases of interest that are not measured by the FTIR include Cl_2 and O_2, which are not active in the IR spectrum, as well as HNO_2.

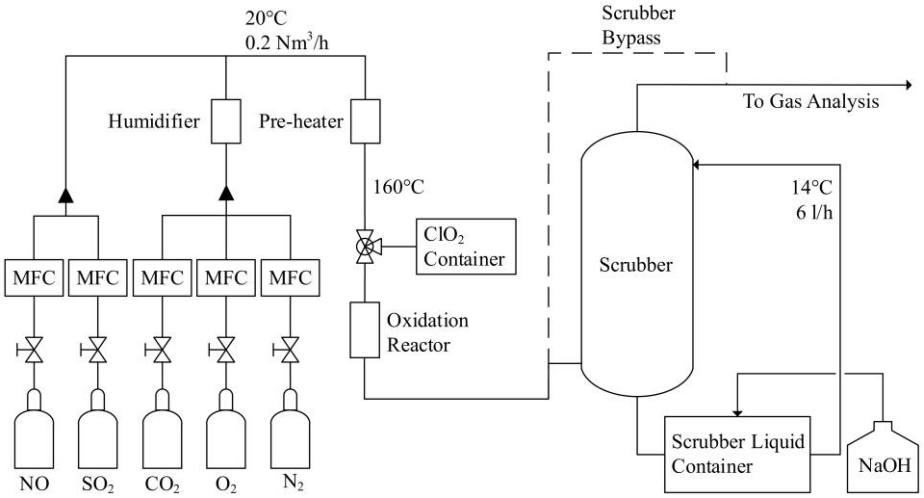

Figure 6: Schematic process outline of the 0.2 Nm^3/h unit. The black line is the gas flow, the solid line indicates the major route, and the dashed line represents a bypass of the scrubber. MFC, Mass flow controller.

Table 1: Investigated parameters and their set values, as used in the 0.2 Nm^3/h unit.

Parameter	Value
Inlet SO_2 concentration	400 ppm
Inlet NO concentration	200 ppm
Inlet O_2 concentration	3%
Inlet CO_2 concentration	10%
Humidifier H_2O levels	0%, 10%, 15%, 25%
Inlet N_2 concentration	Balance
Reactor temperature	160°C
r_{ClO2}	0.2, 0.4, 0.6

5.2 The 100 Nm^3/h Unit

The 100 Nm^3/h unit is displayed in Figure 7. The setup consists of six main parts: the furnace, flue gas cooler, oxidation reactor, ClO_2 generator, scrubber, and scrubber liquid storage and distribution system. Apart from the furnace, which has been described in detail by Andersson et al.,[47] all the parts were designed and constructed for the present investigation. The flue gas cooler was redesigned to facilitate control of the exiting gas temperature within the range of 100°–400°C. The ClO_2 used to oxidize NO to NO_2 is generated in an electrolytic cell from $NaClO_2$ and H_2O using a generator (CDE10; Dioxide Pacific). The generated ClO_2 is diluted with ambient air (up to 3% ClO_2) and injected into the flue gas path through a perforated pipe, which is composed of stainless steel. Immediately after the mixing of the two streams, the flue gas path is widened to function as a reactor in which the oxidation takes place.

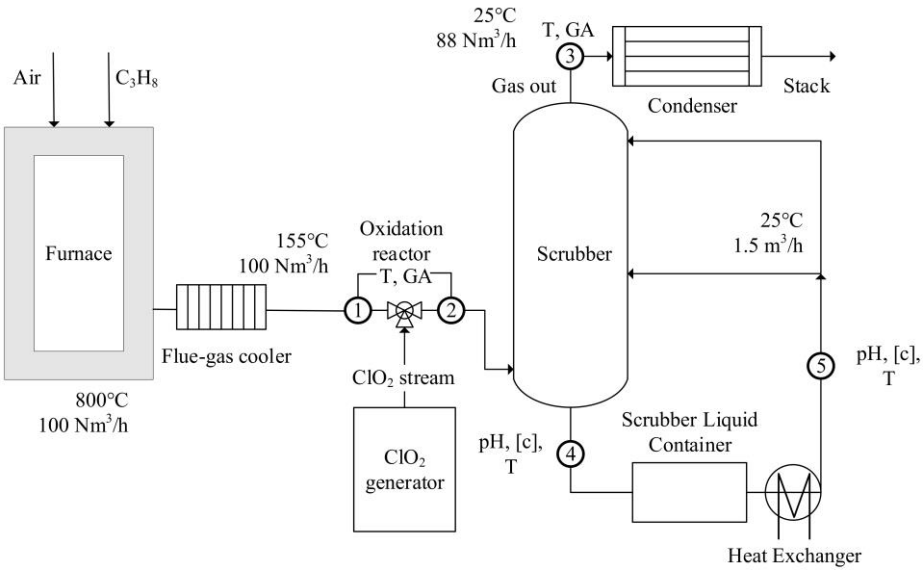

Figure 7: A schematic outline of the process in the 100 Nm^3/h setup. Circles indicate the measurement locations. T, temperature; GA, gas analyzer; pH, scrubber liquid pH level; and [c], scrubber liquid compositions in terms of N(III), N(V) and S(VI).

The diameter of the pipe is expanded via a 200-mm-long cone from 100 mm to 200 mm. The residence time in the reactor is approximately 1 second under standard operating conditions. The flue gas path and the reactor are constructed of stainless steel (SS2343)

After the oxidation reactor, the flue gas enters the scrubber. The scrubber is divided into two sections: a bottom section of height 2.6 m, and a top section of height 1.8 m. The bottom section is a spray tower scrubber with three vertically, evenly distributed inlets fitted with screw nozzles (BETE TF, Hansa Engineering). The bottom section of the scrubber has a diameter of 260 mm and the liquid exits through a drainage port at the very bottom of the reactor. The upper part of the scrubber can be toggled between a spray tower configuration (same specifications as the bottom section and with drainage between the two sections) and a packed bed configuration with diameter of 300 mm and packed height of 2 m.

The packing material used has a metal saddle construction, with a specific surface area of 100 m^2/m^3. The packed bed configuration is supplied with liquid through a screw nozzle at the top. In this configuration, all the liquid exits via the bottom drainage port. The scrubber liquids from the two sections are collected in a tank, in which the pH level is adjusted (based on the pH of the scrubber liquid being fed to the scrubber) by the addition of NaOH (50 wt.%). The scrubber liquid is maintained at 25°C. An installed pump connects to the scrubber liquid feedline and can be used to introduce additives, if so desired.

Table 2: Process parameters evaluated in the 100 Nm^3/h unit, including the wet gas concentrations from the combustion (Position 1 in Figure 7), the ClO_2 added to the oxidation reactor (Position 2), and the scrubber liquid composition (Position 5).

Species	Low limit	High limit
Flue gas composition		
SO_2 (ppm)	0	500
NO (ppm)	70	350
O_2 (vol%)	2.9	7.3
Added oxidizing agent		
r_{ClO2} (mol_{ClO2}/mol_{NO})	0.2	0.4
Scrubber liquid additive		
Na_2SO_3 (g/l)	0	1
Na_2CO_3 (wt.%)	0	10

The gas-phase composition and temperature are measured at three positions in the system (Positions 1, 2, and 3 in Figure 7): before and after the addition of ClO_2 (to establish the rate of oxidation of NO to NO_2), and after the scrubber (to determine the removal efficiency). The flue gas is extracted via Teflon-lined pipes heated to 160°C, and the gas composition is measured in the MultiGas 2030 FTIR Continuous Gas Analyzer. The scrubber liquid can be extracted from the bottom tank, after the pump, as well as from the top and bottom drainage ports. The liquid compositions in the bottom tank and after the pump (what is fed to the scrubber) would ideally be identical assuming perfect mixing. However, there is no forced mixing of the bottom tank. The compositions in terms of N(III), N(V) and S(VI) are measured by ion chromatography. The concentrations of S(IV) in the absorbing liquids of the experiments are difficult to assess since S(IV) oxidizes in the presence of O_2.

The experiments assayed a variety of flue gas compositions and scrubber liquids, as specified in Table 2. As the pH of the scrubber liquid is believed to have a significant impact on the absorption, four pH levels were tested: 1, 5, 7 and 9.[48] As the partial pressure of a gas in an absorption process affects the solubility, according to Henrys law, different gas concentrations of NO_x and SO_x were tested. The presence of SO_2 has also been shown to enhance the absorption of NO_2 through the interaction between S(IV) and N(III), as in Reaction 9. Na_2SO_3 is added directly to the scrubber liquid to increase the rate of Reaction 9, and Na_2CO_3 is added as a buffer to prevent a pH drop. Some experiments were also performed with a decreased flue gas flow (denoted as "reduced flow"), to investigate the effect of increased gas residence time in the scrubber. The flue gas flow in these experiments was 60 Nm^3/h.

5.3 The 400 Nm^3/h Unit

The 400 Nm^3/h unit is illustrated in Figure 8. The setup is, with the exception of the scrubber, enclosed in a 12-meter-long container. Thus, it is a mobile unit that is suitable for field testing at industrial sites. The discussed test was performed at the Källhagsverken plant in Avesta, Sweden. Källhagsverken is a grate-fired waste incineration plant, producing heat for the city of Avesta. The flue gas composition varies with time, owing to variations in the fuel. The 72-hour mean values for the compositions with standard deviations are presented in Table 3. A slipstream is taken from the main flue gas line after the existing NO_x control (SNCR) and PM control (electrostatic precipitator, ESP). The flue gas is transported via insulated steel pipes to the container, where it is connected to Teflon-lined pipes. ClO_2 is injected into the gas stream, and the flue gas composition is analyzed again 8-meters downstream, after which it is fed to a quench. The quench is meant to remove all Cl-containing compounds, to avoid carry-over to the scrubber, so as to prevent corrosion of the equipment and minimize water loss/accumulation in the scrubber as well as to cool the flue gas before the scrubber due to material constraints. The flue gas leaves the quench saturated with water. The scrubber is not cooled and operates at the saturation temperature corresponding to the water content from combustion. The scrubber tower is packed with pall rings (25 mm) and is 4.8 meters in height. The flue gas is transported via a fan back to the main flue gas stream of the plant.

The conditions used for application to a commercial plant differ from those in the controlled experiments, as the process control must consider transient flue gas concentration. The dosing of ClO_2 to the flue gas stream is adjusted in 20-minute intervals based on the average measured NO concentration for the previous two 10-minute periods. This level of control is slow compared to the fluctuations in inlet NO concentration. The ClO_2 feed is set at 20% above the theoretical value for oxidizing the mean NO value (r_{ClO2}=0.48), to balance NO oxidation and ClO_2 consumption.

Table 3: Flue gas composition for the 400 Nm^3/h unit. Shown are the 3-day averages, with standard deviation in parentheses.

Parameter	400 Nm^3/h setup
N_2 (%)	Balance
CO_2 (%)	9.9(1)
H_2O (%)	14.7 (2)
O_2 (%)	5.8 (0.9)
SO_2 (ppm dry)	233 (127)
NO (ppm dry)	72 (20)
CO (ppm dry)	34 (34)

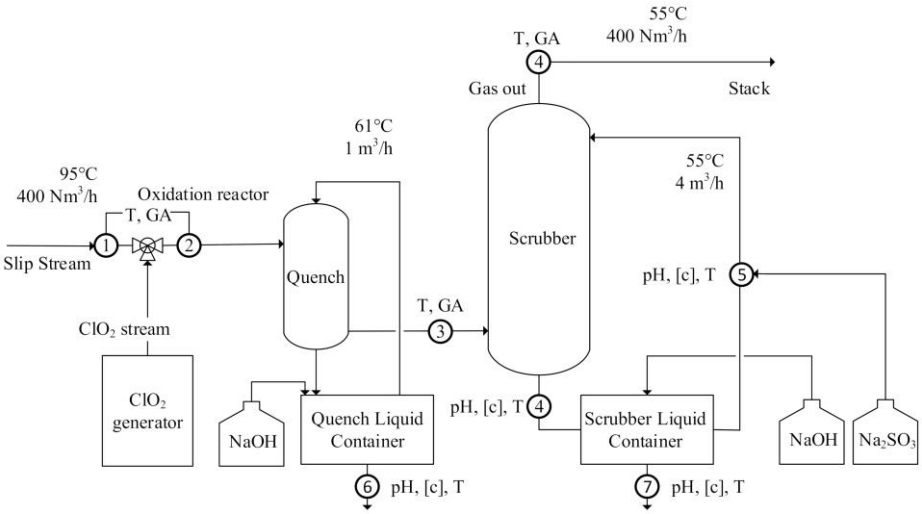

Figure 8: Process outline of the 400 Nm^3/h unit. Circles indicate measurement locations. T, temperature; GA, gas analyzer; pH, pH level; and [c], liquid concentrations.

CHAPTER 6

Modeling

The modeling is based on previous work in our research group by Ajdari, et. al. and the mechanism is described in greater detail in.[27] While the mechanism was developed for the design of pressurized flue gas systems, the reactions are gathered from atmospheric chemistry and as such are within verified conditions. The validation of the reaction mechanism performed herein is a first validation of the compiled model against scrubber experiments. The presence of chloride is completely omitted under the assumption that it will not interfere with the nitrogen and sulfur reactions, except for the inherent influence of the increased ionic strength of the liquid, something which has not yet been studied for this specific case. In any full-scale application, chlorine will most likely be removed in a quench before the scrubber, to avoid the risk of corrosion, which is the case for the 400 Nm^3/h unit in the present work.

All the experimental setups have been modeled using the same reaction mechanism. In the models, the flows and their compositions, as well as the scrubber design are set to describe the experimental setups. However, the experiments are not conducted for long enough to reach steady-state operation with respect to the composition of the absorbing liquid. In the 0.2 Nm^3/h unit, there is not even a bleed-off from the system, although the amount of absorbing liquid is changing with time depending on the water content of the flue gas. Therefore, the simulations are performed with two approaches, Open Loop and Closed Loop simulations, Figure 9 gives an illustration of the process flow for each approach. The Open Loop simulations are used to test the chemistry in the model. The liquid compositions in the experiments are analyzed and the inlet scrubber liquid compositions in the simulations are set to match the measured concentrations. Since there are no measurements of the S(IV) concentration, alternative strategies are used to set the inlet S(IV) concentration in the simulations. Two methods for controlling the S(IV) concentrations in the simulations are used: 1) The amount of S(IV) in the liquid is set to 0, for experiments in which no Na_2SO_3 is added and assuming all the S(IV) is oxidized in the scrubber liquid tank; 2) the S(IV) concentration is set to the theoretical maximum, for experiments in which Na_2SO_3 is added to the inlet liquid feed, either continuously or in batches.

The Closed Loop simulations mimic more accurately the actual operation and evaluate the process performance. It can also be used to assess the Open Loop assumptions with set concentrations. The Closed Loop simulations are performed based on the 400 Nm^3/h unit and with emissions regulations for NO_x and SO_x removal targeted. Since the model only oxidizes S(IV) through reduction of NO_2, the amount of S(IV) accumulates if the S/NO_2 ratio is >0.5. The addition of S to the system is therefore controlled so as to originate either from Na_2SO_3 in the liquid or SO_2 in the flue gas, and the resulting S(IV) concentration is always analyzed as a parameter in the results.

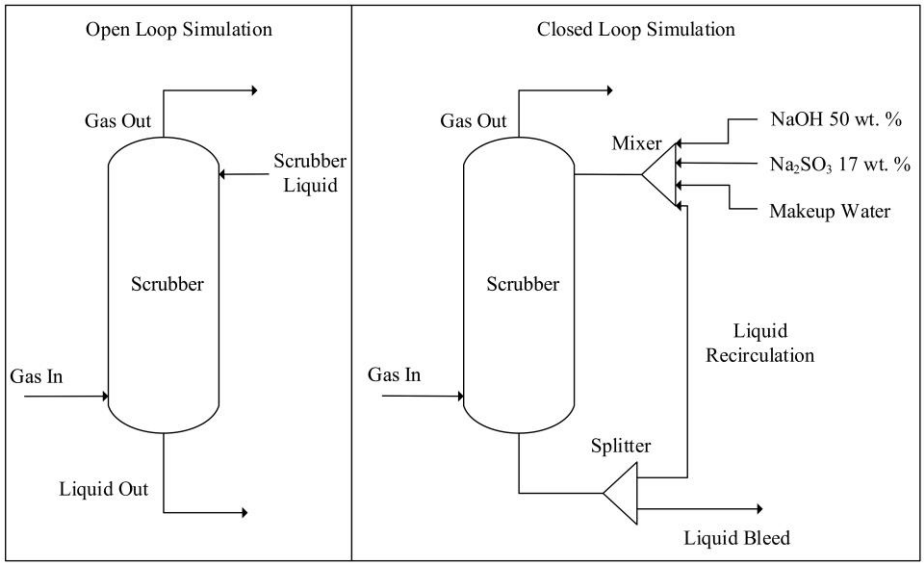

Figure 9: Illustration of the two simulation approaches used: Open Loop (left panel) and Closed Loop (right panel).

CHAPTER 7

Selected Results and Discussion

This chapter summarizes the most important findings of the work of this thesis. The outcomes are collated from the three appended papers, and also include some unpublished results.

7.1 Validation of the Enhanced Oxidation of NO

Figure 10 shows the influence of H_2O on NO conversion. The dashed line represents the theoretical conversion rate of NO to NO_2 when all the ClO_2 reacts exclusively with NO and is reduced to Cl^-, with a stoichiometry of 0.4. The solid line represents the theoretical conversion rate when all the ClO_2 reacts exclusively with NO and is reduced to Cl, with a stoichiometry of 0.5. The results show no major influence of water on NO conversion. It should be noted that there is always some water present in the gas, since the ClO_2 is stripped by N_2 from an aqueous solution. The amount of water is, however, limited to ~0.5%. The oxidation of NO is efficient, with rates that are close to or slightly higher that the dry-basis theoretical conversion rate in all cases.

Figure 11 shows the SO_2 conversion rate, as defined by (4.6), where a negative value indicates that more SO_2 is measured after the oxidation. Comparing the results in

Figure 10 and Figure 11, it is evident that ClO_2 does not oxidize SO_2, while there NO is present for a wide range of water contents. This is vital for the economic feasibility of the concept in that the levels of additives need to be minimized. The very narrow interval (a matter of few ppm) within which the measurements of SO_2 differ can just as well be attributed to measurement detection limits.

The implementation of enhanced oxidation was, after the validation at laboratory scale, evaluated at technical scales, using different materials and nozzle designs. Figure 12 shows the results obtained as NO conversion rate against r_{ClO2}. The 100 Nm^3/h setup delivers the highest conversion at a specific r_{ClO2}, between 0.4 and 0.5, while the 0.2 Nm^3/h and 400 Nm^3/h units have a similar and slightly lower rate of NO conversion at a given r_{ClO2}. All the setups entail the presence of SO_2 in the flue gas, and the 400 Nm^3/h setup has a notable concentration of CO. The results show that ClO_2 is selective towards NO oxidation, even when other reducing species are present, since close to all of the NO is oxidized, as compared to the theoretical maximum. The 0.2 Nm^3/h setup and the 100 Nm^3/h setup are operated at a higher temperature, to avoid condensation in the flue gas train. There is no such control available for the 400 Nm^3/h unit, which is why the flue gas holds the temperature equal to the extracted gas minus the heat lost in the piping.

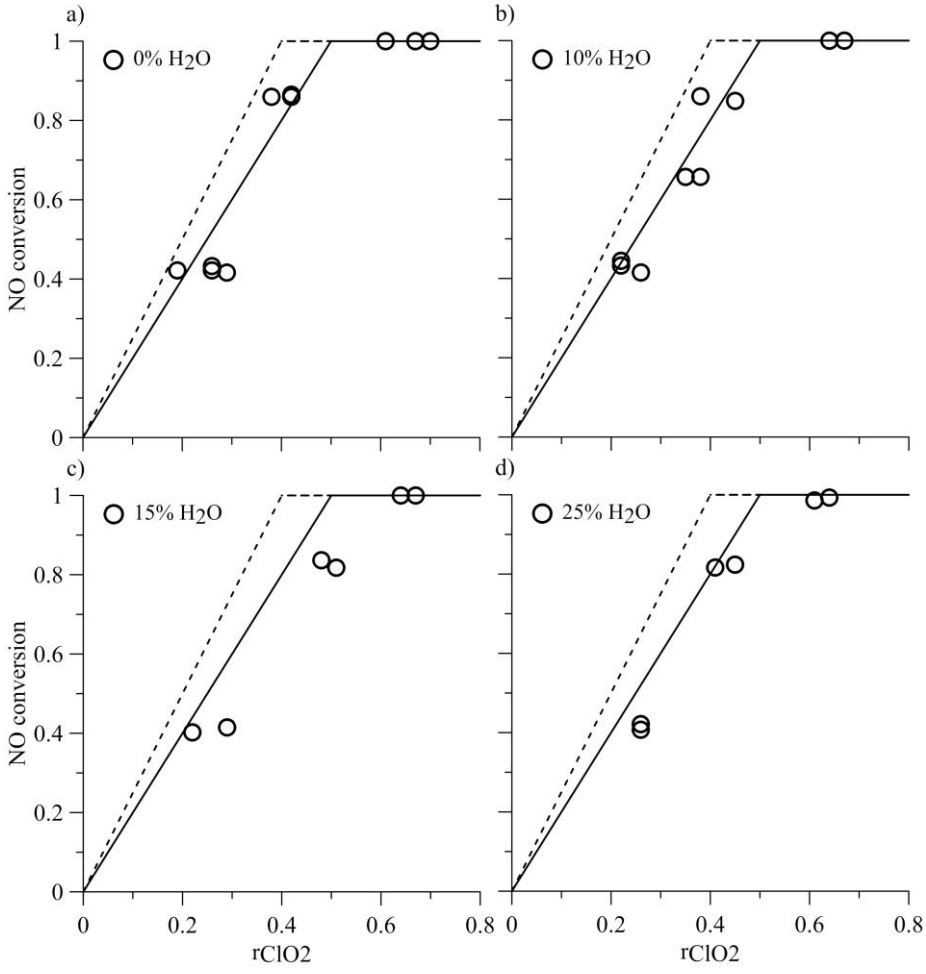

Figure 10: Conversion of NO (as defined by (4.2)) after ClO_2 injection at the humidity levels: (a) 0% H_2O; (b) 10% H_2O; (c) 15% H_2O; and (d) 25% H_2O at the inlet. Measurements are indicated by circles, and the theoretical dry-basis conversion rate is shown with a solid line in each panel. The theoretical wet-basis conversion is indicated with a dashed line in each panel. Experimental conditions were according to Table 1.

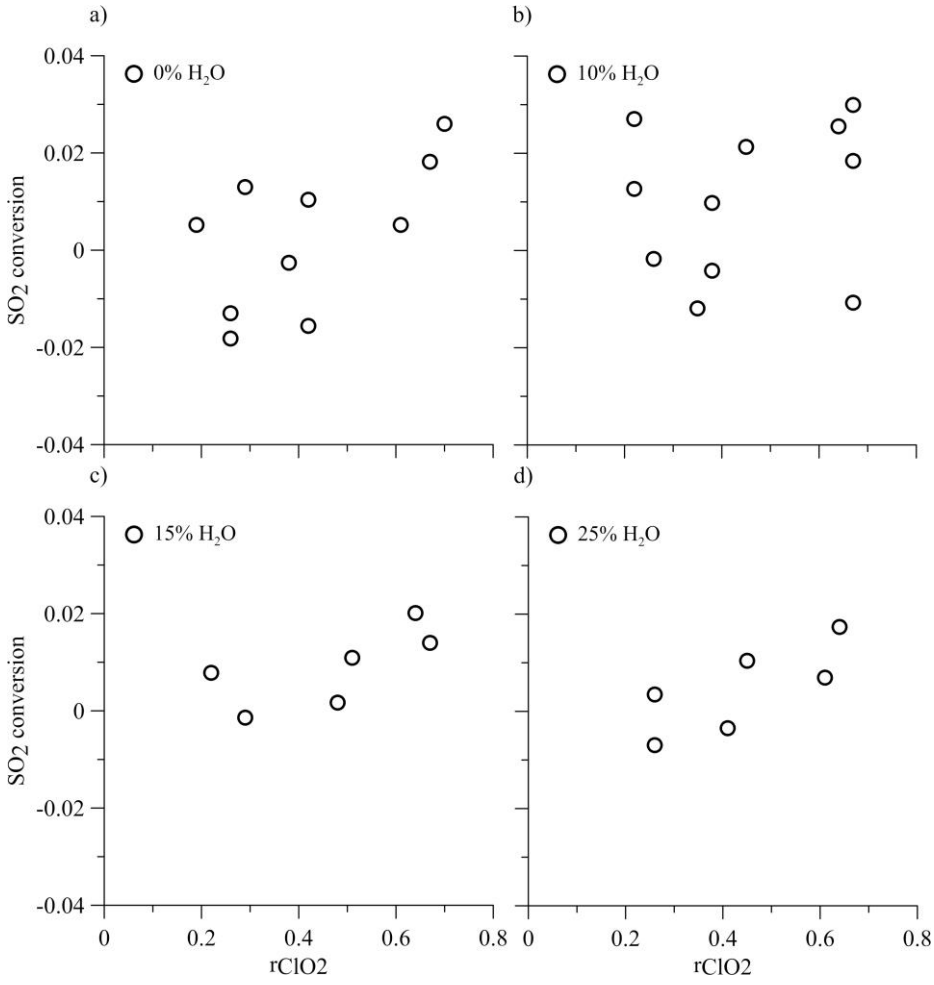

Figure 11: Measured rates of SO_2 conversion (as defined by (4.6)) between experiments with and without ClO_2 injection at different humidity levels: (a) 0% H_2O; (b) 10% H_2O; (c) 15% H_2O; and (d) 25% H_2O at the inlet. The experimental conditions were according to Table 1.

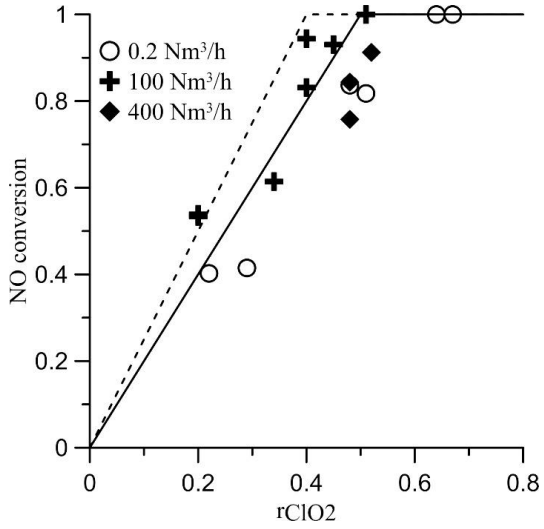

Figure 12: NO conversion rate versus r_{ClO2} (as defined by (4.2) and (4.1) respectively). Comparisons of the 0.2 Nm^3/h, 100 Nm^3/h and 400 Nm^3/h scales. The solid line shows the theoretical NO conversion rate given a stoichiometry of 0.5 for the ClO_2 and NO ratio (Reactions 1 and 2). The dashed line indicates the maximum theoretical conversion rate (Reaction 3). The results for the 0.2 Nm^3/h setup correspond to those shown in Figure 10 c).

An inspection of the oxidation reactor of the 100 Nm^3/h setup was performed after approximately 140 hours of operation. Figure 13 shows the photographs of the reactor from the inspection, together with a color-coded drawing of the oxidation reactor for reference purposes. The bent ClO_2 injection pipe was removed and the opening was used as the entry point for the camera. In general, there are limited signs of corrosion. The most notable sign is in the upper-right image, showing the insertion pipe for the ClO_2 nozzle. The design of this insertion renders it prone to stagnation of the flue gas flow, making it a cold spot. ClO_2 should not be present here, since the nozzle is located downstream of this point. No material samples have been analyzed for a detailed examination of how the environment effects the flue gas path, although these photographs indicate that no high-grade materials are needed for the oxidation reactor so long as the temperatures are kept above the acid dew-point.

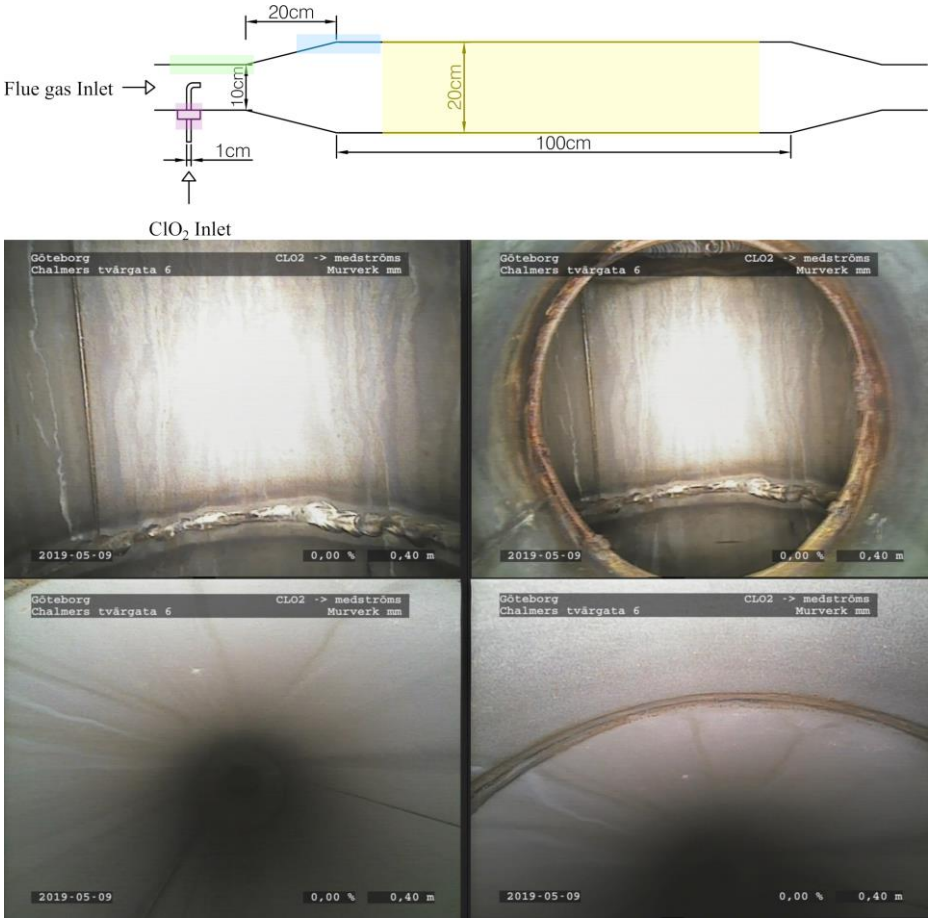

Figure 13: Photographs acquired during the inspection of the oxidation reactor of the 100 Nm^3/h setup, together with color-coded legend. Upper-left panel (green): Pipe wall and welding joint at the start of the pipe expansion from 10-cm to 20-cm diameter. A zoomed view of the upper-right image. Upper-right panel (pink): Pipe wall and welding joint at the start of the pipe expansion, as well as the welding joint for the pipe surrounding the ClO_2 injection nozzle (5-cm diameter). Lower-left panel (yellow): Expanded section of the oxidation reactor. Lower-right panel (blue): Welding joint at the end of the pipe expansion.

7.2 Simultaneous Absorption of NO_x and SO_x

The performance and implementation of the process of simultaneous absorption of NO_x and SO_x were evaluated in the three experimental units and through modeling. As expected, the absorption of SO_2 is efficient in all the setups - <10 ppm of SO_2 at the outlet for all trials with alkaline conditions. Under acidic conditions, the saturation of dissolved SO_2 is approached (after sufficient operational time given the used bleed) and not all SO_2 is absorbed. Figure 14

gives the absorption rates of NO_2 without liquid additives besides pH control for the 0.2 Nm^3/h and 100 Nm^3/h setups. The rate of absorption in the smaller unit is higher. The highest NO_2 absorption (no NO is present) achieved without additives is 78% at pH 10 and with a SO_2 concentration in the flue gas of 1,000 ppm (5-times the NO concentration). The improved absorption seen at higher pH levels with higher SO_2 concentrations is significant, whereas the absorption rate remains almost constant for the other cases in the 0.2 Nm^3/h unit with only a minor influence exerted by the SO_2 concentration. In the 100 Nm^3/h setup, NO_2 absorption is limited (<20%) under acidic conditions. At a pH >7, the NO_2 absorption is improved when the SO_2 concentration in the inlet gas is >400 ppm.

NO formation in the scrubber is detected in the 100 Nm^3/h setup, most likely due to the instability of N(III) at acidic conditions, whereas this is not seen in the 0.2 Nm^3/h unit. At acidic pH, the rate of NO_x absorption, as defined by (4.3), is 6% and 4%, as compared to the NO_2 absorption, defined by (4.4), of 16% and 12% due to NO formation in the scrubber. The highest measured rate of NO_2 absorption for the 100 Nm^3/h setup is 36%, which is seen at 400 ppm of SO_2 and pH of 8.8. This is the only measurement for which there is no reformed NO in the scrubber. The NO_2 absorption is not further improved when increasing the SO_2 concentration at the inlet from 400 to 600 ppm. It should however be noted that there is no continuous analysis of the scrubber liquid composition, why it could be attributed to changes in the scrubber liquid.

Table 4 shows the results obtained from the 0.2 Nm^3/h and 100 Nm^3/h setups when a 17 wt.% solution of Na_2SO_3 is continuously added to the scrubber liquid at a position close to the inlet nozzles. The indicated S(IV) concentration in the liquid is based on the amount added and assuming that no S(IV) accumulates. High rates of absorption of NO_2 are reached in the two setups. Again, formation of NO in the scrubber is seen in the 100 Nm^3/h setup but not in the 0.2 Nm^3/h setup. With the addition of Na_2CO_3 to the scrubber liquid, the formation of NO is decreased; in one experimental case to a point where net absorption of NO is achieved. This indicates that NO is formed from HNO_2 in acidic zones, which are more likely at lower buffering capacity. An alkaline scrubber liquid that has reached steady state should have a fairly limited pH gradient because of all the acid base pairs present, which will likely reduce the rate of NO reformation.

The liquid compositions measured after the experiments are presented in Table 5. The distribution between N(III) and N(V) is almost 1:1. Given the alkaline conditions and that most of the nitrogen is absorbed via Reaction 9, a higher share of N(III) was expected. Oxidation of the nitrogen in the liquid by residual ClO_2 could be an explanation. The amount of residual ClO_2 should however be limited, see Figure 12, and definitely not enough to oxidize the entire amount of nitrogen present. The high concentration of S(VI) is linked to the addition of Na_2SO_3 to the scrubber liquid.

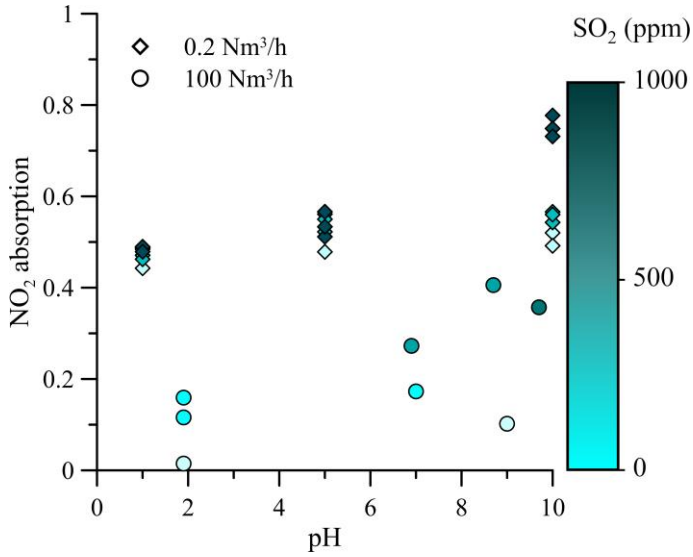

Figure 14: Comparison of NO_x absorption rates, as defined by (4.3), between the 0.2 Nm^3/h and 100 Nm^3/h setups operated at different pH levels and SO_2 gas concentrations. The only additive to the liquid is NaOH for pH control. The three inlet concentrations of SO_2 for the 0.2 Nm^3/h setup are: 0 ppm, 200 ppm, and 1,000 ppm. The four inlet concentrations of SO_2 for the 100 Nm^3/h setup are: 0 ppm, 100 ppm, 400 ppm, and 600 ppm.

Table 4: NO_x absorption profiles for experiments with S(IV) addition to the scrubber liquid inlet conducted in the 0.2 Nm^3/h and 100 Nm^3/h units.

Setup Nm^3/h	τ (s)	S(IV) (g/l)	pH	Na_2CO_3 (wt.%)	NO_2 absorption	NO absorption	NO_x absorption
0.2	6.5	1	9.0	0	91%	0%	91%
0.2	6.5	1	9.0	0	94%	0%	94%
100	9	1	9.5	0	63%	-32%	53%
100	9	1	9.5	0	70%	-94%	59%
100	9	1	8.6	10	71%	-5%	66%
100	15	1	8.8	10	87%	6%	82%
100	9	0.78	7.2	0	85%	-119%	81%
100	9	1.89	7.2	0	74%	-214%	71%

Table 5: Scrubber liquid composition at the completion of the experiments. S(IV) is completely oxidized to S(VI). N(III) is present at a slightly higher concentration than N(V). The pH of the sample was 7.3.

Species	Unit	Result
Cl	mg/l	450
N(III)	mg/l	273
N(V)	mg/l	250
S(VI)	g/l	10

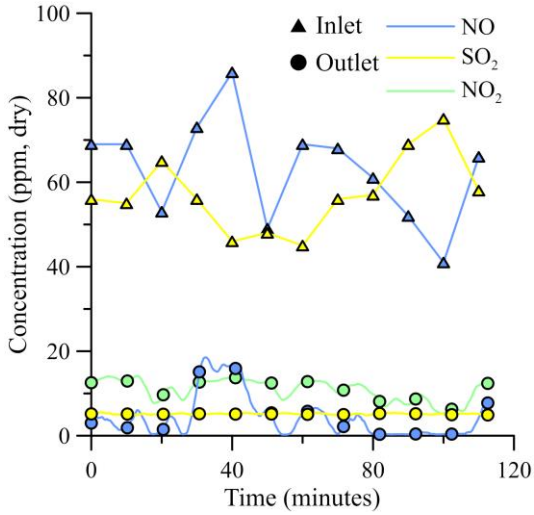

Figure 15: A comparison of the inlet and outlet concentrations of NO, NO_2 and SO_2 during two hours of operation of the 400 Nm^3/h unit. Inlet concentrations are measured before ClO_2 injection, and outlet concentrations are measured after the scrubber. The triangles indicate the inlet streams and the circles indicate the outlet streams. No NO_2 is detected at the inlet (before oxidation). Outlet concentrations are measured every other second while the inlet concentrations are taken as 10-minute interval mean values, i.e. the time resolution is higher for the outlet concentrations.

The absorption concept was evaluated under real-world operational conditions in the 400 Nm^3/h setup. Figure 15 shows the inlet and outlet concentrations of NO, NO_2 and SO_2 for a period of 2 hours of operation of the 400 Nm^3/h unit. There are variations in the inlet concentrations of both NO and SO_2. During the 2 hours of operation, the inlet flow of NO exceeds the amount that it is possible to oxidize with the amount of ClO_2 added over a 20-minute interval, with this occurring after approximately 30 minutes. Otherwise, the NO is completely oxidized in the oxidation reactor. The concentration of NO after the scrubber matches the increase in NO at the inlet, which explains why no absorption of NO seems to take place. The outlet SO_2 concentration remains constant.

The scrubber liquid has a continuous feed of 26 l/h of Na_2SO_3 [127 g/l]. The SO_2 absorption rate remains above 90% and the NO_x absorption rate mostly remains above 80%. The results show that the process, while not optimized, can still control the emissions of NO_x and SO_x continuously. However, it should be noted that the amount of Na_2SO_3 added to the scrubber liquid is high. Since the stoichiometry of Reaction 9 gives a theoretical mole ratio of 0.5 for the S(IV) to NO_2, the added ratio of about 20 is far from optimal.

7.3 Validation of the Reaction Mechanism

The reaction mechanism for simultaneous absorption of NO_x and SO_x previously derived by our research group (see Ajdari et. al.[27]) is compiled from a series of references from various applications, and has not yet been validated for the present application. The evaluation of the reaction mechanism is, thus, an important outcome of the present experimental campaign.

Figure 16 presents the modeling of the 0.2 Nm^3/h setup. For this unit, the mechanism seriously under-predicts the absorption rates, especially under acidic conditions. The model predicts a constant absorption efficiency of approximately 10%, independent of the SO_2 concentration at pH levels <5. At pH levels >5, the influence of the bisulfite interactions starts to improve the absorption. Under alkaline conditions, the influence of SO_2 in the gas phase is considerable in both the simulations and experiments, as is evident when comparing the ~50% absorption in the case with 1,000 ppm of SO_2 to the ~10% absorption in the case without SO_2. The main conclusion drawn from this result is that small-scale scrubbers are difficult to represent with the correlations used in the modeling. The discrepancy between modelling and measurements is, however, in accordance with the difference in NO_2 absorption seen between the 0.2 Nm^3/h unit and the other two setups, which indicates something that cannot be explained by simply comparing process parameters.

In Figure 17, a comparison of the simulation and experimental results from the 100 Nm^3/h unit is shown. The level of agreement between the model predictions and the measurements for this unit is much better than for the laboratory-scale unit. The model, as seen in the results shown in Figure 16, does not capture any influence of SO_2 in the gas phase at pH <5, which explains why all the simulations show an absorber performance that is independent of SO_2 under these conditions. For the experiments conducted under alkaline conditions, the model ably captures the absorption of NO_2. Only one measurement, at pH 8.7, deviates significantly with a simulated absorption of ~30% and an experimental absorption of ~40%. This might be due to as-yet unknown changes in the scrubber liquid, as discussed for Figure 14.

The model does not capture any formation of NO in the scrubber, which is in agreement with the discussion on the importance of local low-pH zones for NO formation as such fluctuations are not present in the model. Reaction 8, which involves N(III) breakdown to NO and NO_2, is favored by high concentrations of N(III) and acidic conditions in the model, which is not seen because the absorption of NO_x, and thereby the concentration of N(III), is limited under acidic conditions. For a liquid with steady-state composition and a more stable pH level throughout the scrubber, little or no NO should be present at the scrubber outlet, which concords with the model. The results indicate that the model is in good agreement with the experimental data in terms of NO_2 absorption and that simulations without recirculation of the scrubber liquid captures the absorption well.

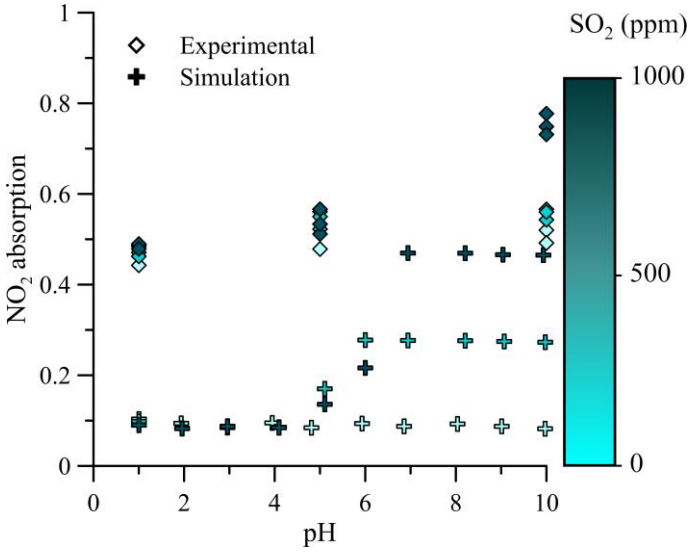

Figure 16: Comparison of the modeling and experimental results presented in Figure 14 for the 0.2 Nm^3/h setup. The three inlet concentrations of SO_2 are: 0 ppm, 200 ppm, and 1,000 ppm. NO_2 absorption is defined by (4.4).

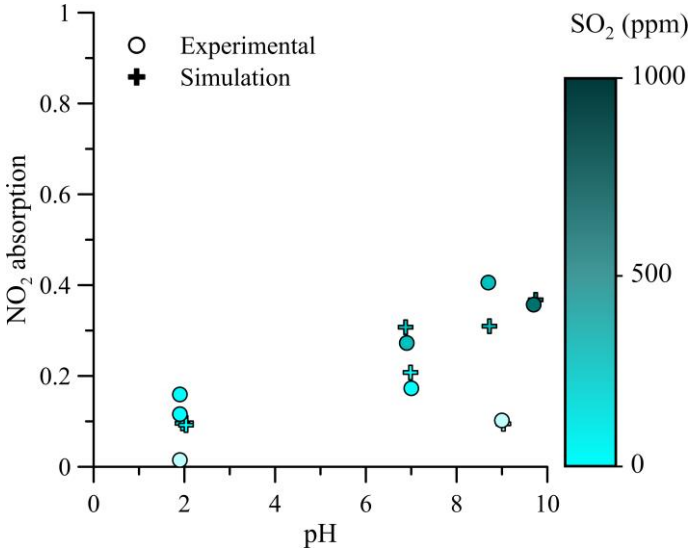

Figure 17: Comparison of the modeling and experimental results presented in Figure 14 for the 100 Nm^3/h setup. The four inlet concentrations of SO_2 are: 0 ppm, 100 ppm, 400 ppm, and 600 ppm. NO_2 absorption is defined by (4.4).

7.4 Modeling of Continuous Operation

To evaluate the composition of the scrubber liquid and the performance of continuous operation, the recirculation make up and bleed streams must be described. As mentioned in Chapter 6, the mechanism does not include a route for S(IV) oxidation [besides that for NO_2(aq) hydrolysis], which results in S(IV) accumulation when the SO_2/NO_2 ratio in the flue gas is >0.5. This phenomenon is, however, not seen in the experiments. Accordingly, an analysis of the simulation results for continuous operation must be performed.

Table 6 presents the compositions of the liquid bleeds for the simulations of the 400 Nm^3/h setup with 240 ppm dry NO_2 and 240 ppm dry SO_2. The predicted absorption rates of NO_2 and SO_2 are 90% and 99%, respectively. The level of liquid bleed is governed by the S(VI) concentration in the scrubber liquid, to avoid the formation of solids. The high concentration of N(III) in the scrubber liquid affects the NO_2 absorption rate negatively. With higher recirculation rates, the concentration of each species increases, including that of S(IV). However, at this operating point the N(III) increase limits the absorption more than the S(IV) increases it. The liquid analysis from the experiments has so far given an N(III)/N(V) ratio between 1–3. The modeling suggests that N(III) is dominating, which is more in line with what is expected under alkaline conditions based on investigations of the proposed chemistry and results for other setups.[15] Under alkaline conditions, the rates of the reactions that form N(V) are limited, and the rate of formation of N(III) from S(IV) is high.

The model performs a sensitivity analysis to investigate the influences of S(IV) concentration and residence time. The experimental results show that the concentration of S(IV) in the absorbing liquid is the single most important parameter for high-level absorption of NO_2. In Figure 18, the NO_2 absorption in the scrubber is plotted against the S(IV) concentration of the absorbing liquid at the inlet. The absorption increases from 14% to 90% when the $S(IV)/NO_2$ ratio increases from 0 to 3.5 (compared to an increase from 0 to 25 in the experimental testing). The amount of S(IV) is controlled through the addition of Na_2SO_3 to the absorbing liquid, and no SO_2 is present in the inlet gas. The sensitivity analysis is performed with a higher bleed compared to Table 6, to make it less computationally expensive.

Table 6: Concentrations of the components of the liquid bleed from the 400 Nm^3/h setup during Closed Loop simulations. The resulting $S(IV)/NO_2$ molar ratio is ~16, with a NO_2 absorption rate of 90%.

Species	N(III)	N(V)	S(IV)	S(VI)	Carbonates
Concentration (mg/l)	20,000	4	860	30,000	43,000

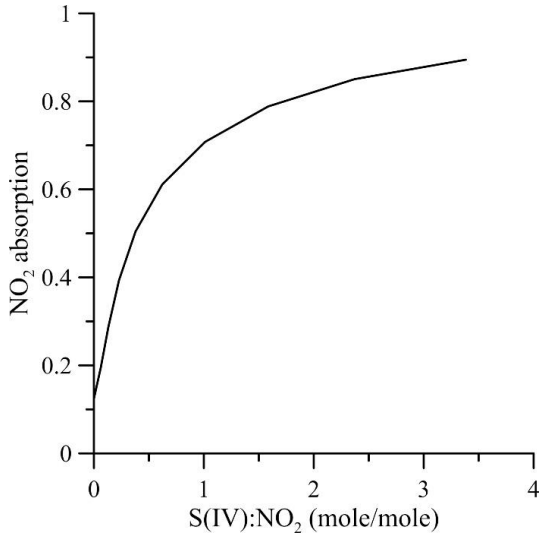

Figure 18: Simulation of the 400 Nm^3/h unit. NO_2 absorption depending on the S(IV) to NO_2 ratio, where S(IV) is measured in the liquid at the top of the scrubber and NO_2 is measured in the inlet gas. NO_2 absorption defined according to (4.4).

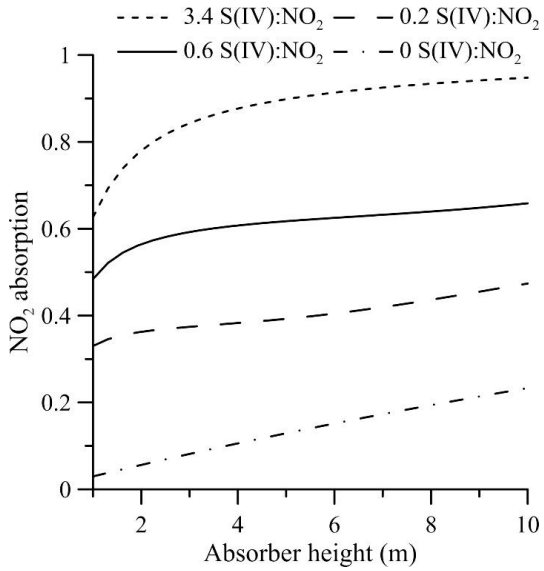

Figure 19: Simulation of the 400 Nm^3/h unit. NO_2 absorption is plotted against scrubber height. Four scrubber liquids are included where the amount of S(IV) compared to the inlet NO_2 is varied from a ratio of 0 to 3.4 mole per mole. NO_2 absorption defined according to (4.4).

In Figure 19, the model evaluates the influences of scrubber height and S(IV) concentration. The height is varied from 1 meter to 10 meters, resulting in the absorption changing from 3% to 93%. The results show the height, i.e., residence time, required for the rate of the S(IV)-NO_2 reaction to decrease, whereinafter the absorption is linearly dependent upon Reactions 6 and 7. The 400 Nm^3/h scrubber has a height of 4.8 meters, which is in the linear segment for all the evaluated concentrations of S(IV), which is a sufficient height for the scrubber to be relatively insensitive to changes.

CHAPTER 8

Conclusions

This work investigates the simultaneous absorption of NO_x and SO_x from flue gases (**Papers II-III**) in a process that employs enhanced oxidation of NO to NO_2 by ClO_2 (**Papers I-III**). The main conclusions drawn from the results of these studies are presented below.

The chemical interactions between a flue gas and ClO_2 at low temperatures (<200°C) has been examined through extensive experiments. It is concluded that NO is efficiently oxidized to NO_2 by ClO_2 gas to achieve complete conversion through fast gas-phase reactions at a ClO_2/NO ratio of ~0.5. This should be compared to the stoichiometric ratio of 0.4 that is required under ideal and wet conditions. Also, the selectivity of ClO_2 towards NO oxidation is high in the investigated environments. There are no indications of SO_2 or CO oxidation in any of the experimental setups. Furthermore, it can be concluded that the concentration of water in the flue gas exerts no effect on the degree to which NO is oxidized.

The absorption of SO_2 is near-complete in all the units under alkaline conditions. For the absorption of NO_2 under alkaline conditions, a consistent trend is noted across the scales: the absorption of NO_2 is increased as the amount of SO_2 is increased in the gas phase or the amount of Na_2SO_3 is increased in the liquid. The results are to a large extent confirmed by the computer modeling of the two larger setups. The most important discrepancy noted in relation to the understanding of the associated chemistries is the rate of S(IV) oxidation in the scrubber tower.

The absorption of NO_2 in the laboratory-scale unit is higher than both the absorption in the larger scale units and the absorption predicted by the modelling for the same conditions. The results of the 0.2 Nm3/h setup is concluded to be not fully representative of the investigated chemistry. Nevertheless, this work establishes that experimental experience relevant for the upscaling and implementation of the investigated concept can be gathered for each of the three setups used. The derived model gives good agreement with the experimental outcomes for the 100 Nm^3/h and 400 Nm^3/h setups, without any extensive parameter fitting.

CHAPTER 9

Suggestions for Future Work

This work has taken the concept of simultaneous absorption of NOx and SOx from theoretical simulations and shown that the concept is possible to scale and that, in large, the proposed understanding of the chemistry describes the process performance and could be used for process design. However, before designing the first full scale demonstration plant this work suggests that further evaluations are made with respect to handling of the scrubber liquid effluent and to the optimization of the scrubber liquid additives to reduce chemical consumption. With respect to the understanding of the liquid-phase chemistry, the oxidation of S(IV) is identified as the main area for future work. Below is a short introduction and some initial ideas on how to approach these areas for future work.

9.1 S(IV) Oxidation

The absorption of NO_2 requires either a very long residence time or a sufficiently high concentration of S(IV) in the scrubber liquid. For this concept to have commercial viability, the oxidation of S(IV) needs to be controlled. Understanding the mechanisms underlying S(IV) oxidation in the presence of NO_2 and O_2, is a critical first step forward. One suggested path forward is to use state-of-the-art measurement equipment to analyze the scrubber chemistry on-line. One potential technique is Raman spectroscopy, which can deliver real-time results for liquid compositions.[49] Since the amount of S(IV) added to the system will strongly influence the process economics, it is vital to understand it´s oxidation and how to control it.

9.2 Scrubber Liquid Effluent Handling

An aspect that is not touched upon in this work but that needs to be addressed is the handling of the scrubber liquid effluent. The absorption concept itself is proven, and the fact that there are several different potential end-users makes this an interesting and challenging task. Several approaches to waste treatment could potentially be adopted, such as:

- Refining sulfur to sulfuric acid and nitrogen to nitric acid.
- Produce nitrates as fertilizers or to reduce nitrite to N_2.[50]
- Recirculation of scrubber liquid effluent to the combustion step, to reduce nitrogen to N_2 and potentially reduce part of the S(VI) to SO_2 which would benefit the absorption of NO_2 in the scrubber.

Bibliography

(1) EEA *Every breath we take. Improving air quality in Europe*; 2013.
(2) Masson-Delmotte, V., P. Zhai, H.-O. Pörtner, D. Roberts, J. Skea, P.R. Shukla,; A. Pirani, W. M.-O., C. Péan, R. Pidcock, S. Connors, J.B.R. Matthews, Y. Chen, X. Zhou, M.I. Gomis,; E. Lonnoy, T. M., M. Tignor, and T. Waterfield (eds.) *Summary for Policymakers*; IPPC: 2018.
(3) EEA Air pollutant emissions data viewer (Gothenburg Protocol, LRTAP Convention) 1990-2017. https://www.eea.europa.eu/data-and-maps/dashboards/air-pollutant-emissions-data-viewer-2 (2020-01-23),
(4) WHO, *Ambient air pollution: A global assessment of exposure and burden of disease"*. 2016.
(5) EEA *Air quality in Europe - 2019 report*; 10/2019; EEA: 2019.
(6) IEA World energy balance and statistics. https://www.iea.org/data-and-statistics (2020-01-23),
(7) Layr, K.; Hartleib, P., Market Analysis for Urban Mining of Phosphogypsum. *Berg Huettenmaenn Monatsh* **2019,** 164, (6), 245-249.
(8) Oskarsson, K.; Berglund, A.; Deling, R.; Snellman, U.; Stenbäck, O.; Fritz, J. J., A Planner's Guide for Selecting Clean-Coal Technologies for Power Plants. In *World Bank Technical paper NO. 367*, The World Bank: 1997.
(9) Senjo, T.; Kobayashi, M., Process for removing nitrogen oxides from gas. In Google Patents: 1976.
(10) Littlejohn, D.; Chang, S. G., Removal of Nox and So2 from Flue-Gas by Peracid Solutions. *Ind Eng Chem Res* **1990,** 29, (7), 1420-1424.
(11) White, V.; Torrente-Murciano, L.; Sturgeon, D.; Chadwick, D., Purification of oxyfuel-derived CO2. *Int J Greenh Gas Con* **2010,** 4, (2), 137-142.
(12) Liemans, I.; Alban, B.; Tranier, J. P.; Thomas, D., SOx and NOx absorption based removal into acidic conditions for the flue gas treatment in oxy-fuel combustion. *Enrgy Proced* **2011,** 4, 2847-2854.
(13) Kasper, J. M.; Clausen, C. A.; Cooper, C. D., Control of nitrogen oxide emissions by hydrogen peroxide-enhanced gas-phase oxidation of nitric oxide. *J Air Waste Manage* **1996,** 46, (2), 127-133.
(14) Sun, W. Y.; Ding, S. L.; Zeng, S. S.; Su, S. J.; Jiang, W. J., Simultaneous absorption of NO_x and SO_2 from flue gas with pyrolusite slurry combined with gas-phase oxidation of NO using ozone. *J Hazard Mater* **2011,** 192, (1), 124-130.
(15) Heijnesson Hulten, A.; Nilsson, P.; Samuelsson, M.; Ajdari, S.; Normann, F.; Andersson, K., First evaluation of a multicomponent flue gas cleaning concept using chlorine dioxide gas - Experiments on chemistry and process performance. *Fuel* **2017,** 210, 885-891.
(16) Johansson, J.; Normann, F.; Sarajlic, N.; Andersson, K., Technical-Scale Evaluation of Scrubber-Based, Co-Removal of NOx and SOx Species from

Flue Gases via Gas-Phase Oxidation. *Ind Eng Chem Res* **2019,** 58, (48), 21904-21912.
(17) Shen, C. H.; Rochelle, G. T., Nitrogen dioxide absorption and sulfite oxidation in aqueous sulfite. *Environ Sci Technol* **1998,** 32, (13), 1994-2003.
(18) Adewuyi, Y. G.; He, X. D.; Shaw, H.; Lolertpihop, W., Simultaneous absorption and oxidation of NO and SO2 by aqueous solutions of sodium chlorite. *Chem Eng Commun* **1999,** 174, 21-51.
(19) Chien, T. W.; Chu, H., Removal of SO2 and NO from flue gas by wet scrubbing using an aqueous NaClO2 solution. *J Hazard Mater* **2000,** 80, (1-3), 43-57.
(20) Jin, D. S.; Deshwal, B. R.; Park, Y. S.; Lee, H. K., Simultaneous removal of SO_2 and NO by wet scrubbing using aqueous chlorine dioxide solution. *J Hazard Mater* **2006,** 135, (1-3), 412-417.
(21) Richardson, R. G., Removal of atmospheric pollutants from gas, related apparatuses, processes and uses thereof. In Google Patents: 2016.
(22) Parrish, C. F.; Chung, L., Control of emissions. In Google Patents: 2013.
(23) Sun, C. L.; Zhao, N.; Wang, H. Q.; Wu, Z. B., Simultaneous Absorption of NO_x and SO_2 Using Magnesia Slurry Combined with Ozone Oxidation. *Energ Fuel* **2015,** 29, (5), 3276-3283.
(24) Trainer, J. P.; Court, P.; Darde, A.; Perrin, N., CO2 Purification Unit for Oxy-Coal Combustion Systems. In *1st International Oxyfuel Combustion Conference Cottbus*, Germany, 2009.
(25) Shah, M.; Degenstein, N.; Zanfir, M.; Kumar, R.; Bugayong, J.; Burgers, K., Near Zero Emissions Oxy-Combustion CO2 Purification Technology. *Enrgy Proced* **2011,** 4, 988-995.
(26) Normann, F.; Jansson, E.; Petersson, T.; Andersson, K., Nitrogen and sulphur chemistry in pressurised flue gas systems: A comparison of modelling and experiments. *Int J Greenh Gas Con* **2013,** 12, 26-34.
(27) Ajdari, S.; Normann, F.; Andersson, K.; Johnsson, F., Reduced Mechanism for Nitrogen and Sulfur Chemistry in Pressurized Flue Gas Systems. *Ind Eng Chem Res* **2016,** 55, (19), 5514-5525.
(28) EU, Directive 2016/802. In 2016.
(29) MEPC, Revised MAPOL Annex VI. In 2008.
(30) Naturvårdsverket *Miljöavgift på utsläpp av kväveoxider från energiproduktion år 2018 - resultat och statistik*; 2019.
(31) Atkinson, R.; Baulch, D. L.; Cox, R. A.; Hampson, R. F.; Kerr, J. A.; Rossi, M. J.; Troe, J., Evaluated kinetic, photochemical and heterogeneous data for atmospheric chemistry .5. IUPAC Subcommittee on Gas Kinetic Data Evaluation for Atmospheric Chemistry. *J Phys Chem Ref Data* **1997,** 26, (3), 521-1011.
(32) Atkinson, R.; Baulch, D. L.; Cox, R. A.; Hampson, R. F.; Kerr, J. A.; Rossi, M. J.; Troe, J., Evaluated kinetic and photochemical data for atmospheric chemistry: Supplement VIII, halogen species - IUPAC Subcommittee on Gas

Kinetic Data Evaluation for Atmospheric Chemistry. *J Phys Chem Ref Data* **2000,** 29, (2), 167-266.
(33) Demore, W. B.; Sander, S. P.; Golden, D. M.; Hampson, R. F.; Kurylo, M. J.; Howard, C. J.; Ravishankara, A. R.; Kolb, C. E.; Molina, M. J. *Chemical Kinetics and Photochemical Data for Use in Stratospheric Modeling*; Jet Propulsion Laboratory, 1997.
(34) Watson, R. T., Rate Constants for Reactions of Clox of Atmospheric Interest. *J Phys Chem Ref Data* **1977,** 6, (3), 871-917.
(35) Beyad, Y.; Burns, R.; Puxty, G.; Maeder, M., A speciation study of sulfur(IV) in aqueous solution. *Dalton T* **2014,** 43, (5), 2147-2152.
(36) Siddiqi, M. A.; Krissmann, J.; PetersGerth, P.; Luckas, M.; Lucas, K., Spectrophotometric measurement of the vapour-liquid equilibria of (sulphur dioxide plus water). *J Chem Thermodyn* **1996,** 28, (7), 685-700.
(37) Voegele, A. E.; Tautermann, C. S.; Loerting, T.; Hallbrucker, A.; Mayer, E.; Liedl, K. R., About the stability of sulfurous acid (H2SO3) and its dimer. *Chem-Eur J* **2002,** 8, (24), 5644-5651.
(38) Rhee, J. S.; Dasgupta, P. K., The second dissociation constant of sulfur dioxide-water. *J Phys Chem-Us* **1985,** 89, (9), 1799-1804.
(39) Schwartz, S. E., Equilibria in the Nitrogen-Oxide Nitrogen Oxyacid-Water System. *Abstr Pap Am Chem S* **1980,** 180, (Aug), 221-Phys.
(40) Lee, Y. N.; Schwartz, S. E., Reaction-Kinetics of Nitrogen-Dioxide with Liquid Water at Low Partial-Pressure. *J Phys Chem-Us* **1981,** 85, (7), 840-848.
(41) Park, J. Y.; Lee, Y. N., Solubility and Decomposition Kinetics of Nitrous-Acid in Aqueous-Solution. *J Phys Chem-Us* **1988,** 92, (22), 6294-6302.
(42) Clifton, C. L.; Altstein, N.; Huie, R. E., Rate-Constant for the Reaction of No2 with Sulfur(Iv) over the Ph Range 5.3-13. *Environ Sci Technol* **1988,** 22, (5), 586-589.
(43) Littlejohn, D.; Wang, Y. Z.; Chang, S. G., Oxidation of Aqueous Sulfite Ion by Nitrogen-Dioxide. *Environ Sci Technol* **1993,** 27, (10), 2162-2167.
(44) Sapkota, V. N. A.; Fine, N. A.; Rochelle, G. T., NO2-Catalyzed Sulfite Oxidation. *Ind Eng Chem Res* **2015,** 54, (17), 4815-4822.
(45) Sun, Y.; Hong, X. W.; Zhu, T. L.; Guo, X. Y.; Xie, D. Y., The Chemical Behaviors of Nitrogen Dioxide Absorption in Sulfite Solution. *Appl Sci-Basel* **2017,** 7, (4).
(46) Zhuang, Z.; Sun, C.; Zhao, N.; Wang, H.; Wu, Z., Numerical simulation of NO2 absorption using sodium sulfite in a spray tower. *Journal of Chemical Technology & Biotechnology* **2016,** 91, (4), 994-1003.
(47) Andersson, K.; Johansson, R.; Iohnsson, F.; Leckner, B., Radiation intensity of propane-fired oxy-fuel flames: Implications for soot formation. *Energ Fuel* **2008,** 22, (3), 1535-1541.
(48) Ajdari, S.; Normann, F.; Andersson, K.; Johnsson, F., Modeling the Nitrogen and Sulfur Chemistry in Pressurized Flue Gas Systems. *Ind Eng Chem Res* **2015,** 54, (4), 1216-1227.

(49) Jinadasa, M. H. W. N. Process analytical technology for real-time quantitative speciation of aqueous phase CO2 capture solvents. USN, 2019.
(50) Winkler, F.; Schoedel, N.; Zander, H. J.; Ritter, R., Cold DeNOx development for oxyfuel power plants. *Int J Greenh Gas Con* **2011,** 5, S231-S237.